

Open Access

# Comparative Study of the Compressive Strength of Different Commercial Graphite Grades at Room and High Temperatures

Michele Ballan<sup>1\*</sup>, Stefano Corradetti<sup>1</sup>, Lisa Centofante<sup>1</sup>, Alberto Monetti<sup>1</sup>, Mattia Manzolaro<sup>1,2</sup> and Giovanni Meneghetti<sup>2</sup>

<sup>1</sup>Legnaro National Laboratories, National Institute of Nuclear Physics, Legnaro 35020, Italy.

<sup>2</sup>Department of Industrial Engineering, University of Padua, Padua 35131, Italy.

\*Correspondence to: Michele Ballan, Legnaro National Laboratories, National Institute of Nuclear Physics, Legnaro 35020, Italy. Email: [michele.ballan@lnl.infn.it](mailto:michele.ballan@lnl.infn.it)

Received: May 9, 2023; Accepted: August 14, 2023; Published Online: August 25, 2023

Citation: Ballan M, Corradetti S, Centofante L, Monetti A, Manzolaro M and Meneghetti G. Comparative Study of the Compressive Strength of Different Commercial Graphite Grades at Room and High Temperatures. *Advanced Materials Science and Technology*, 2023;5(1):0515557. <https://doi.org/10.37155/2717-526X-0501-4>

**Abstract:** Graphite is often employed for several high temperature research and industrial applications, thanks to its refractoriness and its physical properties such as high thermal conductivity, low thermal expansion and excellent thermal shock resistance. However, its mechanical properties at high temperatures are often unknown and are strongly influenced by its microstructure and composition. This work is focused on a comparative analysis of the compressive strength up to 2000°C of three different commercial graphite grades provided by TOYO TANSO. Two grades of the same kind but different density, IG-43 and IG-45, and a grade with finer grains, TTK-4, were considered. Such materials were selected as their nominal physical and chemical properties are suitable for withstanding the extreme working conditions typical of nuclear applications characterized by high temperature, high vacuum and radiation damage. For the performance of the compressive tests, a custom-built vacuum experimental equipment was used, capable of resistively heating conductive samples at a temperature level up to 2000°C. Specimens with an hourglass shape were manufactured and tested in triplicate at room-temperature, 1000°C and 2000°C for each type of graphite. The dependence of the compressive strength on the graphite grade density and microstructure was highlighted, resulting in higher resistance for denser grades, in accordance with data reported by the supplier. Results collected for the room-temperature tests were consistent with the material datasheets, whereas at 2000°C, an increase of approximately 30%-40% of the compressive strength was displayed compared to its room-temperature value.

**Keywords:** Graphite; Compressive strength; High temperature; Hourglass-shaped specimen



© The Author(s) 2023. **Open Access** This article is licensed under a Creative Commons Attribution 4.0 International License (<https://creativecommons.org/licenses/by/4.0/>), which permits unrestricted use, sharing, adaptation, distribution and reproduction in any medium or format, for any purpose, even commercially, as long as you give appropriate credit to the original author(s) and the source, provide a link to the Creative Commons license, and indicate if changes were made.

## 1. Introduction

High temperature research and industrial applications often require the employment of materials capable of withstanding extreme working conditions. An example is provided by graphite, which is characterized by an excellent thermal shock resistance thanks to its high resistance at high temperature, low thermal expansion and high thermal conductivity. Typical state-of-art industrial applications of graphite are the metallurgical or renewable energy industries, where, for instance, it is selected as construction material of crucibles or furnaces. However, it is also candidate material in several cutting-edge fields, such as aerospace or nuclear physics for accelerator facilities. A couple of examples of the latter topic are provided by the SPES ISOL (Selective Production of Exotic Species-Isotope Separation On-Line) facility<sup>[1-3]</sup> and the RD\_MUCOL (R&D on MUon COLLinders) experiment<sup>[4]</sup>.

SPES is an accelerator facility, currently in the installation phase at Legnaro National Laboratories of INFN, Italy, aimed at the production of radioactive ion beams useful for nuclear physics and medical research<sup>[3,5,6]</sup>. Several core components of the SPES system work in an extremely harsh environment, characterized by high vacuum ( $10^{-6}$  mbar), temperature levels above 2000 °C and high radiation doses, undergoing severe thermal stresses<sup>[7-9]</sup>. Considering such working conditions, graphite represents one of the best choices for the design and manufacture of several devices at SPES<sup>[10]</sup>.

RD\_MUCOL is an INFN experiment aimed at preparing the ground for the installation of the Muon Collider, a future accelerator experiment at CERN with the scope to exploit muon collisions for discoveries and precision measurements at high energies. The realization of such complex accelerator requires to overcome technological challenges with extensive theoretical and experimental studies, and graphite materials are investigated as promising targets for muon production in future colliders<sup>[11]</sup>.

Several kinds of graphite are available in the market, differing in microstructure, grain size, grain orientation and density. However, such material variety results in a dispersion of its physical properties, in particular mechanical and thermal properties. Furthermore, in

many cases such information is not available in the mentioned temperature range. On the other hand, the aforementioned nuclear physics experiments require the knowledge of the material physical properties in the working temperature range, particularly in the design phases to predict the behavior of target materials in the operational environment<sup>[12]</sup>. In particular, restrained thermal expansions induce compressive stresses, that could compromise their structural integrity and lead to the experiment interruption or, in the worst cases, the need for a human intervention, adding a risk of exposure to a radiation dose.

As highlighted in various literature studies<sup>[13-16]</sup>, the tensile and compressive strength of all tested graphite grades is strongly temperature dependent and it increases up to 2500 °C, where the maximum performance is observed and in some cases, it resulted twice the room temperature compressive strength. Furthermore, compressive strength is also dependent on the material density, where higher values are exhibited for denser graphite grades. In addition, it was observed that even the minor density fluctuations typical of different batches of the same graphite grade resulted in appreciable variations of the measured compressive strength<sup>[16]</sup>.

In such context, the aim of the present work is to evaluate and compare the high temperature (up to 2000 °C) compressive strength of three types of isotropic ultrafine grain graphite produced by TOYO TANSO, namely IG-43, IG-45 and TTK-4. Such materials are good candidates for the development of nuclear physics devices, however, to date, there are not data available regarding their high temperature compressive strength. To estimate the compressive strength a custom experimental set-up developed at INFN-LNL was employed following the previous successful tests with the POCO EDM-3 graphite<sup>[16,17]</sup>.

## 2. Materials and Methods

### 2.1 Materials

The grades of TOYO TANSO graphite considered in this study are IG-43, IG-45 and TTK-4. They are isotropic ultrafine graphite, IG-43 and IG-45 being very similar in microstructure, but different in density, and IG-45 slightly denser. TTK-4 has a different microstructure, which was specifically developed for the EDM manufacture of complex shapes such

as honeycomb and ultra-fine surfaces or multi-cavity molds. **Table 1** reports relevant thermo-physical and

mechanical properties reported in the datasheet<sup>[18]</sup>.

**Table 1.** Material properties provided by the TOYO TANSO datasheet for the selected graphite grades

Grade	Average grain size/ $\mu\text{m}$	Bulk density/ $\text{g}\cdot\text{cm}^{-3}$	Shore Hardness/HSD	Electrical resistivity/ $\mu\Omega\text{m}$	Flexural strength/MPa	Compressive strength/MPa	Tensile strength/MPa	Young's modulus/GPa	Coefficient of thermal expansion/ $10^{-6}\cdot\text{K}^{-1}$	Thermal conductivity/ $\text{W}\cdot(\text{mK})^{-1}$
IG-43	10	1.82	55	9.2	54	90	37	10.8	4.8	140
IG-45	10	1.88	55	9	60	110	40	12	4.9	140
TTK-4	4	1.78	72	14	73	135	49	10.9	5	90

For each type of graphite, 20 mm diameter rods were purchased, and samples were machined in a lathe. The hourglass specimen geometry was selected as reported in **Figure 1**, in accordance with the tests performed on the POCO EDM-3, where several sample geometries had been investigated<sup>[16]</sup>. The hourglass shape outperformed the others as failure always started at the reduced cross section, where a nearly pure uniaxial compression exists. A total of 9 samples for each graphite grade were produced, by extracting them from different positions of the rod.

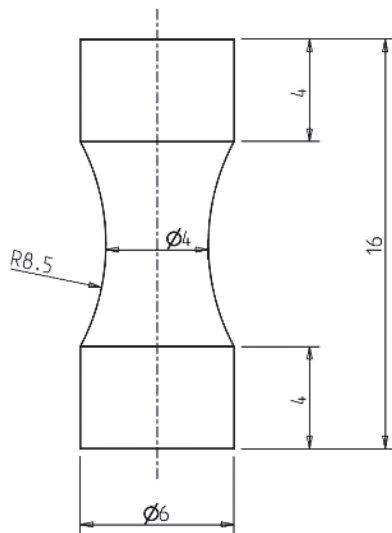


**Figure 1.** The hourglass specimen geometry for the compression tests. Dimensions are in mm

## 2.2 Density Measurement

Bulk density measurements on all produced hourglass samples were performed for verifying both the material uniformity and the data declared by the supplier. The Archimedes approach was adopted, according to the ISO standard procedure for the determination of density and apparent porosity of fine ceramics<sup>[19]</sup>. A commercial Sartorius YDK01 kit for the Sartorius ME235P scale was employed.

## 2.3 Compressive Tests

Compressive tests were performed with a custom experimental set-up, reported in **Figure 2**. Such test bench is described in detail in previous studies<sup>[16,17]</sup>, to which the reader is referred and consists of an aluminum vacuum chamber, where a high vacuum level up to  $10^{-5}$  mbar is created. Vacuum is fundamental for the high temperature testing of the graphite specimens, as the material rapidly degrades under atmospheric conditions if the temperature is higher than  $800\text{ }^{\circ}\text{C}$ <sup>[20]</sup>.

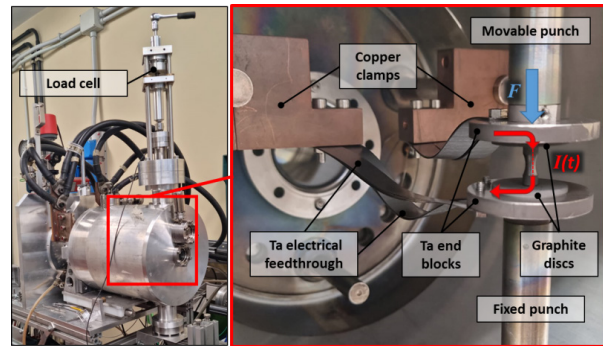


**Figure 2.** The experimental set-up used for the compressive tests

The graphite specimen is placed on top of a fixed punch, and is pressed with a manually actuated movable punch. For the high temperature tests, graphite discs are interposed between the specimen and the tantalum end blocks, in order to avoid material deterioration. Such disks were made with TTK-4 graphite, which exhibits the highest hardness, as reported in **Table 1**.

Both punches are made of stainless steel and are electrically insulated with ceramic current breaks placed at the opposite extremity of the punch shaft respect to the tantalum end blocks. In such way, it is possible to resistively heat the sample feeding a DC current directly to the other extremity of the punches. Such extremities present a tantalum ending, in order to withstand the high temperature levels reached during the tests. The current is fed to the punches by means of

tantalum flexible foils, connected to a couple of water cooled cylindrical copper feedthroughs by means of copper clamps, as displayed in **Figure 2**.

The movable punch is connected to a bellow, allowing its axial translation without compromising the vacuum level inside the vacuum chamber. Compressive forces are measured by means of an HBM-U9C 10 kN tension-compression load cell installed by means of two threaded connections between the movable punch and the manual actuator. Such device consists of a leadscrew gear, which converts the manual handle rotation into a linear motion. Therefore, the torque applied to the handle is transferred to the specimen as a compressive load. Furthermore, the vacuum chamber is equipped with a Kodial® viewport in correspondence of the sample to enable the temperature measurements at the specimen center by means of infrared pyrometers (IRCON® modline 5 R, Fluke Process Instrument, Everett, WA) during the tests.

Tests at room temperature were performed in atmospheric environment, since vacuum was not necessary to prevent the sample degradation. On

the other hand, vacuum was necessary for all tests at high temperature which were performed at two temperatures, namely 1000 °C and 2000 °C. During the high temperature tests the vacuum level of  $10^{-5}$  mbar was first achieved, and then the heating current was slowly and gradually tuned until the pyrometer readout displayed the desired temperature level. For all considered materials, three samples for each temperature were tested.

After the tests, the specimen fragments were collected and the fracture surfaces were observed with a Scanning Electron Microscope (SEM - TESCAN model VEGA 3) to visually assess fracture surfaces.

### 3. Results and discussion

#### 3.1 Density Measurement

**Table 2** reports the comparison between the bulk density reported in the datasheet and measured with the Archimedes for the three graphite grades considered. Data collected in the present investigation are reported as mean values and standard deviations.

**Table 2.** comparison between the bulk density provided by the TOYO TANSO datasheet and measured in this investigation for the selected graphite grades

Grade	Bulk density (datasheet)/g·cm <sup>-3</sup>	Bulk density (this work)/g·cm <sup>-3</sup>
IG-43	1.82	1.81±0.02
IG-45	1.88	1.89±0.05
TTK-4	1.78	1.79±0.01

**Table 2** highlights that all measured bulk density values are consistent with the data provided by the supplier and, since samples were extracted from different positions of the same bar, the material homogeneity was also verified.

#### 3.2 Compressive Tests

Consistently with the observation performed in the case of the POCO EDM-3 hourglass specimens<sup>[16]</sup>, failure patterns were difficult to observe. The specimens often broke abruptly, and even though failure always started at the reduced cross section at the center of the sample, two or three large fragments were generated, with some smaller chips. The largest pieces were retrieved for SEM observations.

In this study, data for the compressive strength are presented in the form of the ratio  $F_r/A$ , that represents the engineering compressive strength. Hence, the cross

section area “A” adopted for the calculation of the  $F_r/A$  ratios corresponds to the minimum net-section diameter of 4 mm reported in Figure 1 which was measured for all specimens individually with an accuracy of 0.01 mm. However, all graphite grades are prone to plastic deformation and therefore the true compressive strength  $F_r/A_t$  referred to the minimum cross section is not feasible. In fact,  $A_t$  is the true minimum cross section at the failure which is greater than A owing to the combined effects of plastic and elastic deformation. The estimation of  $A_t$  would require the implementation of a dedicated measurement system, i.e. a computer vision system, capable of monitoring the sample diameter increase during the test.

However, it is relevant to highlight that the reported engineering  $F_r/A$  ratios represent a reasonable approximation of the actual true compressive strength.

In a previous work a Poisson ratio of approximately 0.14 was estimated for a similar isotropic graphite grade manufactured by the same producer<sup>[21]</sup>. Additionally, compressive deformation studies performed on the same kind of nuclear-grade isotropic graphite reported a 3%-4% strain at the fracture<sup>[22,23]</sup>. Provided that the graphite grades considered in this study are expected to exhibit a similar behavior, the difference between

the true and the engineering compressive strength should be approximately between 1% and 2%, which is reasonably negligible.

The measured compressive strength for the three graphite grades at room temperature (RT), 1000 °C and 2000 °C are reported in **Figure 3** and **Table 3**. In **Figure 3**, data are reported with the corresponding 99.7% confidence level error bars.

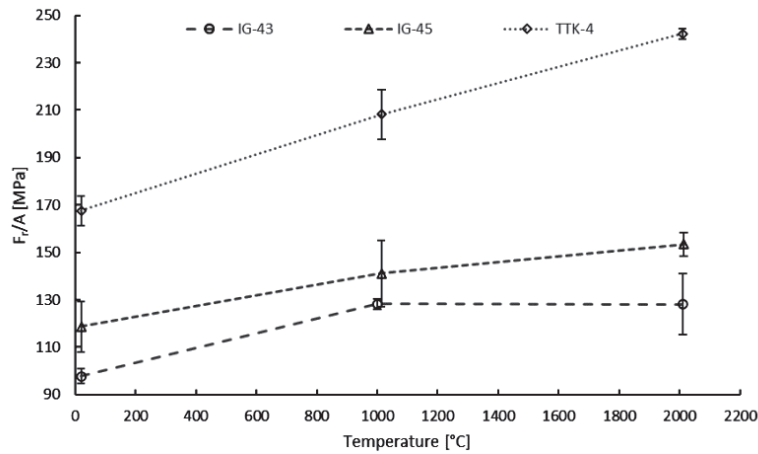


**Figure 3.** trend of compressive strengths of three graphite grades at the three temperature levels

In addition, datasheet information of the compressive strength for each material are reported in Table 3 for a quantitative comparison. The datasheet compressive strengths are generally lower but consistent with the measured engineering  $F_r/A$  ratios. It is however possible to observe that IG-43 exhibits the lowest compressive strength, whereas the highest values were measured for the TTK-4 grade, consistently with the information reported by the supplier. Additionally,

in the case of both IG-43 and IG-45, the 2000 °C compressive strength increases of around 30% respect to the room temperature value. On the other side, for the TTK-4 grade, the 2000 °C compressive strength raises approximately 45% in comparison with the room temperature measurements. To the best of authors' knowledge, the present data are the first published regarding compressive strength at 1000 °C and 2000 °C for the graphite grades considered in this investigation.

**Table 3.** Compressive strength collected at the three temperature levels for the three graphite grades and comparison with the datasheet room temperature values. Measurements performed in this study are reported with the calculated 99.7% confidence limits

Grade	Compressive strength (datasheet) <sup>*</sup> /MPa	Experimental compressive strength $F_r/A$ (this work)/MPa		
	RT	RT	1000 °C	2000 °C
IG-43	90	98±3	128±2	128±12
IG-45	110	118±11	141±14	153±5
TTK-4	135	167±6	208±10	242±3

<sup>\*</sup>Datasheet values report the compressive ultimate strength provided by the supplier

The effect of density can be highlighted comparing the results for IG-43 and IG-45, IG-45 being 3% denser. Indeed, consistently with previous studies, IG-45 exhibits a compressive strength approximately 20% higher. A very similar effect was also observed

for the POCO EDM-3 graphite, where a variation of 3% in density produced an increase of 20% in compressive strength<sup>[16]</sup>. On the other side, the effect of a finer microstructure can be emphasized comparing the results for IG-43 and TTK-4. Although IG-43 is

slightly denser than TTK-4 ( $1.82 \text{ g/cm}^3$  compared to  $1.78 \text{ g/cm}^3$  for TTK-4), its compressive strength is 1.5 times lower. As declared by the supplier, TTK-4 has an average grain size of  $4 \mu\text{m}$ , which is significantly than the declared grain size for the IG grades ( $10 \mu\text{m}$ ). This outcome suggests that also a finer microstructure has a significant positive effect on the compressive strength.

**Figure 4** displays some representative examples of the SEM observations performed on the fracture surfaces of the specimens tested at the three temperature levels for IG-43, IG-45 and TTK-4. As expected according to the supplier specifications, it is possible to observe that TTK-4 has a finer microstructure compared to IG-43 and IG-45. In addition, in the case of the TTK-4 grade, the SEM

images taken at the different temperature levels often exhibited regions with a slightly distorted grains. Such effect might be due to the occurrence of plastic strains. Previous studies remark that polycrystalline graphite structures, anisotropy, inelastic micro-cracking, and plastic slippage at crystalline interfaces cause marked nonlinearity in the mechanical properties, and finite values of residual plastic deformation can be observed after unloading the specimen<sup>[24,25]</sup>. The finer microstructure of TTK-4 is characterized by a larger density of crystalline interfaces, that may enhance the aforementioned effects related to plastic strain, leading to a slightly more evident ductility of the material, especially at higher temperature, where higher loads are required to induce the specimen fracture.

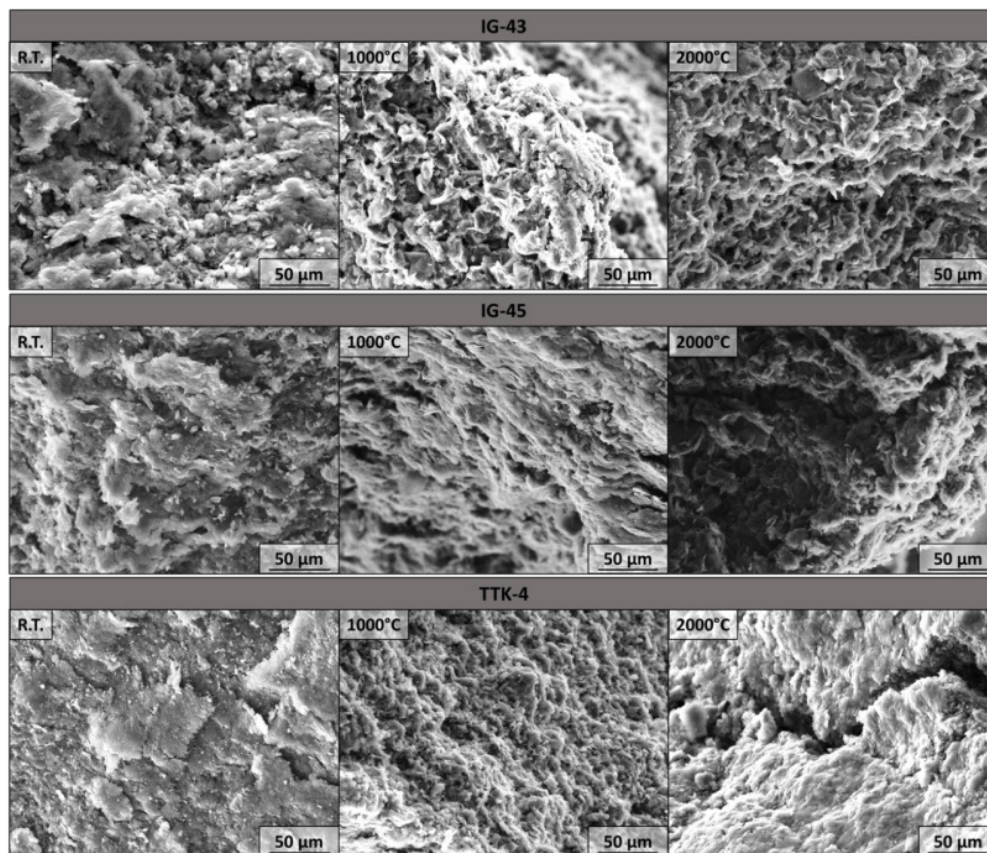


**Figure 4.** Representative SEM picture of the fracture surfaces for the IG-43, IG-45 and TTK-4 samples tested at environmental temperature (R.T.), 1000 °C and 2000 °C

#### 4. Conclusion

This study presents the comparative compressive tests performed at room and high temperature on three types of isotropic ultrafine grade graphite produced by TOYO TANSO, namely IG-43, IG-45 and TTK-

4. Density for each material was measured and values consistent with the supplier datasheet were observed. The compression test results showed in all cases an increase of the engineering compressive strength over temperature. IG-43 was confirmed as the least resistant,

whereas the highest compressive strengths were found for TTK -4 in accordance with the supplier's datasheet. In the case of IG-43 and IG-45, the load necessary for fracturing the sample at 2000 °C was 30% higher compared to room temperature; as to TTK-4 materials, approximately a 45% increment was observed. The effect of density, in accordance with literature data, could be observed comparing IG-43 with IG-45. The latter is 3% denser and exhibits a compressive strength approximately 20% higher. The effect of a finer microstructure played also a role and could be observed comparing IG-43 grade with TTK-4, where the latter material is the least dense but exhibited a 1.5 higher compressive strength than the IG-43 thanks to its finer microstructure.

As a future outlook, if true stress-strain curves at each temperature were experimentally determined (i.e. with other room temperature and high temperature compressive tests), the calculation of the stress distribution at the failure would be feasible for instance with a simple finite element model<sup>[26]</sup>. In such case, the true compressive strength would be determined from the stress evaluation at the most critical location, applying an appropriate yield criterion, as Tresca or Von Mises<sup>[17,27]</sup>.

### Author's Contributions

Conceptualization: Manzolaro M, Corradetti S and Meneghetti G

Methodology: Centofante L, Monetti A and Meneghetti G

Validation: Manzolaro M, Corradetti S, Ballan M and Meneghetti G

Investigation: Ballan M

Resources: Manzolaro M and Corradetti S

Data curation: Manzolaro M, Ballan M and Meneghetti G

Writing-original draft preparation: Ballan M

Writing-review and editing: Centofante L, Ballan M, Monetti A and Meneghetti G

Visualization: Manzolaro M and Corradetti S

Supervision: Manzolaro M and Meneghetti G

Project administration: Manzolaro M

Funding acquisition: Corradetti S

All authors have read and agreed to the published version of the manuscript.

### Ethics Statement

Not applicable.

### Consent for publication

Not applicable.

### Availability of Supporting Data

Not applicable.

### Conflict of Interest

The authors declare no conflict of interest.

### Copyright

© The Author(s) 2023.

### References

- [1] Andrighetto A, Manzolaro M, Corradetti S, *et al.* Spes: an intense source of neutron-rich radioactive beams at Legnaro. *Journal of Physics: Conference Series*, 2018;966(1):012028. <https://doi.org/10.1088/1742-6596/966/1/012028>
- [2] Marchi T, Prete G, Gramegna F, *et al.* The SPES facility at Legnaro National Laboratories. *Journal of Physics: Conference Series*, 2020;1643(1):012036. <https://doi.org/10.1088/1742-6596/1643/1/012036>
- [3] Corradetti S, Manzolaro M, Carturan SM, *et al.* The SPES target production and characterization. *Nuclear Instruments and Methods in Physics Research Section B: Beam Interactions with Materials and Atoms*, 2021;488:12-22. <https://doi.org/10.1016/j.nimb.2020.12.003>
- [4] Boscolo M, Delahaye JP and Palmer M. The future prospects of muon colliders and neutrino factories. *Reviews of Accelerator Science and Technology*, 2019;10(01):189-214. <https://doi.org/10.1142/S179362681930010X>
- [5] Andrighetto A, Tosato M, Ballan M, *et al.* The ISOLPHARM project: ISOL-based production of radionuclides for medical applications. *Journal of Radioanalytical and Nuclear Chemistry*, 2019;322:73-77. <https://doi.org/10.1007/s10967-019-06698-0>
- [6] Ballan M, Tosato M, Verona M, *et al.* Preliminary evaluation of the production of non-carrier added <sup>111</sup>Ag as core of a therapeutic radiopharmaceutical in the framework of ISOLPHARM\_Ag experiment. *Applied Radiation and Isotopes*, 2020;164:109258. <https://doi.org/10.1016/j.apradiso.2020.109258>
- [7] Monetti A, Bark RA, Andrighetto A, *et al.* On-line test using multi-foil SiC target at iThemba LABS.

- The European Physical Journal A*, 2016;52:1-10.  
<https://doi.org/10.1140/epja/i2016-16168-0>
- [8] Ballan M, Manzolaro M, Meneghetti G, *et al.* A combined experimental and numerical approach for the control and monitoring of the SPES target during operation at high temperature. *Nuclear Instruments and Methods in Physics Research Section B: Beam Interactions with Materials and Atoms*, 2016;376:28-32.  
<https://doi.org/10.1016/j.nimb.2016.01.038>
- [9] Manzolaro M, Corradetti S, Ballan M, *et al.* Thermal and mechanical characterization of carbides for high temperature nuclear applications. *Materials*, 2021;14(10):2689.  
<https://doi.org/10.3390/ma14102689>
- [10] Monetti A, Andrighetto A, Petrovich C, *et al.* The RIB production target for the SPES project. *The European Physical Journal A*, 2015;51:1-11.  
<https://doi.org/10.1140/epja/i2015-15128-6>
- [11] Boscolo M, Antonelli M, Ciarma A, *et al.* Muon production and accumulation from positrons on target. *Physical Review Accelerators and Beams*, 2020;23(5):051001.  
<https://doi.org/10.1103/PhysRevAccelBeams.23.051001>
- [12] Cesarini G, Antonelli M, Anulli F, *et al.* Theoretical modeling for the thermal stability of solid targets in a positron-driven muon collider. *International Journal of Thermophysics*, 2021;42:1-27.  
<https://doi.org/10.1007/s10765-021-02913-x>
- [13] Wagner P and Driesner AR. High-temperature mechanical properties of graphite. I. creep in compression. *Journal of Applied Physics*, 1959;30(2):148-151.  
<https://doi.org/10.1063/1.1735123>
- [14] Malmstrom C, Keen R and Green L. Some mechanical properties of graphite at elevated temperatures. *Journal of Applied Physics*, 1951;22(5):593-600.  
<https://doi.org/10.1063/1.1700013>
- [15] Gillin LM. Deformation characteristics of nuclear grade graphites. *Journal of Nuclear Materials*, 1967;23(3):280-288.  
[https://doi.org/10.1016/0022-3115\(67\)90160-2](https://doi.org/10.1016/0022-3115(67)90160-2)
- [16] Centofante L, Monetti A and Meneghetti G. High temperature compression tests of a commercial isotropic ultrafine grain graphite. *Advanced Materials Science and Technology*, 2020;2(1): 45-45.  
<https://doi.org/10.37155/2717-526X-0201-5>
- [17] Centofante L, Monetti A and Meneghetti G. High temperature biaxial compressive strength of a commercial isotropic ultrafine grain graphite. *IOP Conference Series: Materials Science and Engineering*, 2021;1038(1):012037.  
<https://doi.org/10.1088/1757-899X/1038/1/012037>
- [18] TOYO TANSO® Isotropic Graphite Property Data. Available from:  
[https://www.toyotanso.com/Products/Special\\_graphite/data.html](https://www.toyotanso.com/Products/Special_graphite/data.html)
- [19] ISO 18754:2020 Fine ceramics (advanced ceramics, advanced technical ceramics) - Determination of density and apparent porosity. Available from:  
<https://www.iso.org/standard/69745.html>
- [20] Xiaowei Luo X, Robin JC and Yu S. Effect of temperature on graphite oxidation behavior. *Nuclear Engineering and Design*, 2004;227(3):273-280.  
<https://doi.org/10.1016/j.nucengdes.2003.11.004>
- [21] Carroll MC. *Initial comparison of baseline physical and mechanical properties for the VHTR candidate graphite grades*. Idaho Falls: Idaho National Lab.(INL), 2014. Available from:  
<https://ndmas.inl.gov/Graphite/Initial%20Comparison%20of%20Baseline%20Physical%20and%20Mechanical%20Properties%20for%20the%20VHTR%20Candidate%20Graphite%20Grades.pdf>
- [22] Yoda S, Eto M and Oku T. Change in dynamic young's modulus of nuclear-grade isotropic graphite during tensile and compressive stressing. *Journal of Nuclear Materials*, 1983;119(2-3): 278-283.  
[https://doi.org/10.1016/0022-3115\(83\)90204-0](https://doi.org/10.1016/0022-3115(83)90204-0)
- [23] Yoda S, Eto M, Tanaka K, *et al.* Effects of oxidation on compressive deformation behavior of nuclear-grade isotropic graphite. *Carbon*, 1985;23(1):33-38.  
[https://doi.org/10.1016/0008-6223\(85\)90193-9](https://doi.org/10.1016/0008-6223(85)90193-9)
- [24] Johns S, Windes WE, Rohrbaugh DT, *et al.* High temperature annealing of irradiated nuclear grade graphite. *Journal of Nuclear Materials*, 2023;579:154377.  
<https://doi.org/10.1016/j.jnucmat.2023.154377>

- [25] Sakai M, Urashima K and Inagaki M. Energy principle of elastic-plastic fracture and its application to the fracture mechanics of a polycrystalline graphite. *Journal of the American Ceramic society*, 1983;66(12):868-874. <https://doi.org/10.1111/j.1151-2916.1983.tb11003.x>
- [26] Chebac R, Vanoni F, Porta A, *et al.* A multidisciplinary approach to optimizing the mechanical characterization and dismantling of nuclear-grade graphite. *Carbon Trends*, 2023;10:100253. <https://doi.org/10.1016/j.cartre.2023.100253>
- [27] Iyoku T, Shiozawa S, Ishihara M, *et al.* Graphite core structures and their structural design criteria in the HTTR. *Nuclear Engineering and Design*, 1991;132(1):23-30. [https://doi.org/10.1016/0029-5493\(91\)90291-O](https://doi.org/10.1016/0029-5493(91)90291-O)